

Biochemical and Ultrastructural Lung Damage Induced by Rhabdomyolysis in the Rat

RAMÓN RODRIGO,^{*,1} SERGIO TRUJILLO,[†] AND CLEOFINA BOSCO[‡]

**Molecular and Clinical Pharmacology Program, Institute of Biomedical Sciences, Faculty of Medicine, University of Chile, Santiago, Chile; †National Institute of Thorax, Medical Surgical Service, Santiago, Chile; and ‡Anatomy and Biology of Development Program, Institute of Biomedical Sciences, Faculty of Medicine, University of Chile, Santiago, Chile.*

Rhabdomyolysis-induced oxidative stress is associated with morphological and functional damage to the kidney and other organs, but applications of this model in the lung are still lacking. The aim of the present study was to determine the relationship between oxidative stress and the morphological changes occurring in the lungs of rats subjected to rhabdomyolysis. Rhabdomyolysis was induced by intramuscular glycerol injection (50% v/v, 10 ml/kg), and the control group was injected with saline vehicle. Arterial blood samples were drawn at 0, 2, 4, and 6 hrs for measurement of arterial gases, creatine kinase activity, and plasma free F₂-isoprostane levels. Six hours later, the lungs were removed to determine the wet-to-dry weight ratio, reduced glutathione (GSH) and GSH disulfide (GSSG) levels, and activity of antioxidant enzymes (catalase [CAT], superoxide dismutase [SOD], and GSH peroxidase [GSH-Px]). Protein carbonylation and lipid peroxidation were assessed in the lungs by measurement of carbonyl and malondialdehyde (MDA) production, respectively. Bronchoalveolar lavage, cell counts, and lung ultrastructural studies were also performed. Six hours after glycerol injection, arterial PO₂ and PCO₂ were 23% and 38% lower, respectively, and plasma free F₂-isoprostane levels were 72% higher, compared with control values. In lungs, protein carbonyl and MDA production were 58% and 12% higher, respectively; the GSH:GSSG ratio and GSH-Px activity were 43% and 60% lower, respectively; and activities of CAT and SOD showed no significant differences compared with controls. Rhabdomyolysis-induced ultrastructural impairment of the lung showed Type II cell damage, extracytoplasmic lamellar bodies and lack of tubular myelin

reorganization, endothelial cellular edema, and no disruption of the alveolar-capillary barrier. These results provide evidence that rhabdomyolysis could induce tissue injury associated with increased oxidative stress, suggesting the contribution of oxidative stress to the pathogenic mechanism of acute lung injury.

Key words: antioxidant enzymes; glutathione; F₂-isoprostanes; lung; rhabdomyolysis

Introduction

Acute respiratory distress syndrome (ARDS) may be caused by pulmonary and nonpulmonary diseases, including sepsis, severe pneumonia, peritonitis, and multiple trauma (1, 2); it is characterized by an overwhelming inflammatory reaction of the pulmonary parenchyma. In ARDS, the lung shows an increase in neutrophils (3, 4) and proinflammatory cytokines, including interleukin-1 (IL-1) and tumor necrosis factor- α (5). Also, products of inflammatory cell activation, like the neutrophil protease enzymes elastase (6) and collagenase (7), are found within the alveolar air space. In addition, elastase and alveolar IL-8 are reported to be augmented in the circulation of patients with ARDS (8). The occurrence of oxidative stress is thought to be involved in the pathogenesis of the lung injury found in different settings, such as hyperoxia (9, 10), acute and chronic ethanol intoxication (11), and ozone exposure or certain drug effects (12). Moreover, elevated plasma F₂-isoprostane levels, recognized as reliable biomarkers of oxidative stress (13, 14), have been shown to be predictive of mortality in patients with ARDS (13, 15). Also, increased F₂-isoprostane levels in exhaled air have been reported (15). Depletion of reduced glutathione (GSH), the most prevalent intracellular thiol, in alveolar epithelial lining fluid is a characteristic finding in patients with ARDS (16). Experimental animal models of acute lung injury (ALI) include two mechanisms of insults, indirectly by the blood (e.g., endotoxin) (17) or directly by the airways (e.g., HCl instillation) (18).

This research was supported by grant 1040429 from the Fondo Nacional de Desarrollo Científico y Tecnológico.

¹ To whom correspondence should be addressed at Molecular and Clinical Pharmacology Program, Institute of Biomedical Sciences, Faculty of Medicine, University of Chile, Independencia 1027, Casilla 70058, Santiago 7, Chile. E-mail: rodrigo@med.uchile.cl

RHABDOMYOLYSIS-INDUCED LUNG INJURY

Rhabdomyolysis, causing acute renal injury (19, 20) by a mechanism partly mediated by oxidative stress (21), could damage other organs such as the lung, which has not been considered in this setting, to our knowledge. It is known that heme iron-induced oxidative stress plays a role in renal tubular cytotoxicity (22). Ferritin levels are increased in patients with multiple traumas, and ferritin iron may worsen the oxidative damage to the lung in ALI (22). However, further studies of the mechanism by which rhabdomyolysis might be involved in alveolar epithelial damage are needed. The aim of the present study was to assess the association between rhabdomyolysis-induced oxidative stress and the resulting biochemical functional and ultrastructural effects on the lung.

Materials and Methods

Animals and Experimental Procedures. Adult male Wistar albino rats (*Rattus norvegicus*) weighing 200 g to 250 g (Institute of Biomedical Sciences, Faculty of Medicine, University of Chile) were given free access to pellet chow (Champion, Santiago, Chile) and water before the experiments. Management of rats was carried out according to internationally accepted ethical rules. The rats were deprived of water for 12 hrs. Then, under light ether anesthesia, both hind limbs of the rat were injected with 50% glycerol in saline (total dose, 10 ml/kg, im), and the animals (n = 68) were allowed free access to water (23). The control rats were injected with an equal volume of normal saline (n = 68) and finally were anesthetized with sodium pentobarbital (40 mg/kg, ip).

Functional Studies. Wet-to-Dry Weight Ratio Analysis. Six hours after glycerol or saline injection, the lungs of 24 rats from each group were harvested. The left lung was dried to a constant mass in an oven kept at 50°C. The wet-to-dry weight ratio was then determined (24), and the right lung was used for ultrastructural studies.

Bronchoalveolar Lavage (BAL) Cell Count. To harvest the pulmonary cells for morphological and functional analysis, 12 rats from each group were killed at 6 hrs after glycerol injection with an overdose of sodium pentobarbital and exsanguination. BAL was performed with calcium-free and magnesium-free phosphate-buffered saline (pH 7.4). The first BAL volume was administered as 2 ml per 100 g of body wt. This volume was placed into the lungs *via* a tracheal cannula for 30 secs with light massage, withdrawn, and again instilled into the lungs for 30 secs more. The recovered fluid was then centrifuged at 300 g for 10 mins (25).

After pooling the BAL samples, the total numbers of cells were counted in a hemocytometer. To obtain neutrophil and macrophage counts, the samples were centrifuged. BAL samples were stained with Wright and Giemsa solutions. Differential counts were performed on 200 cells using standard morphological criteria. Protein concentration was determined in the supernatant of the

lavaged fluid for 10 mins at 4°C by the method of Lowry *et al.* (26).

Blood Gases. Blood samples of eight rats from each group were drawn at 0, 2, 4, and 6 hrs after glycerol injection. Additional pentobarbital sodium (25 mg/kg) was administered every hour. A blood sample was drawn from the carotid artery after cannulation with a Silastic catheter (Silastic medical-grade tubing, 0.305-mm i.d., 0.635-mm o.d.). Body temperature was continuously monitored *via* a rectal probe and was maintained at 37°C with thermostatically controlled plates. The PO₂ and PCO₂ were determined using an ABL 5 (Radiometer, Copenhagen, Denmark) blood gas analyzer.

Biochemical Assays. For biochemical studies, at 6 hrs after glycerol injection eight rats from each group were subjected to an infusion *via* jugular vein with Earle's mineral essential medium (Sigma-Aldrich, St. Louis MO) containing sodium bicarbonate (2.2 g/l, pH 7.40). Perfusate was passed through the vascular bed to remove residual blood at a rate of 40 ml/kg of body wt per minute (23). The lungs were excised and immediately placed in ice-cold 0.25 M sucrose, blotted on filter paper, weighed, and homogenized as indicated for each assay. Homogenates were prepared either in 0.25 M sucrose to determine superoxide dismutase (SOD, EC 1.15.1.1) activity (27) or in 1.15% KCl-0.010 M Tris (pH 7.40) to determine the activities of both catalase (CAT, EC 1.11.1.6) (28) and GSH peroxidase (GSH-Px, EC 1.11.1.9) (29). Reduced GSH and GSH disulfide (GSSG) were assayed by fluorometry, according to the method of Hissin and Hilf (30). Furthermore, the GSH:GSSG ratio was calculated. Plasma antioxidant capacity was measured according to the method of Benzie and Strain (31) by determination of the ferric-reducing ability of plasma (FRAP), which was expressed as micromoles per liter. Plasma levels of uric acid, a major contributor to the antioxidant capacity of plasma, were also measured. The assay for lipid peroxide products was performed in plasma and lung tissue. Lung lipid peroxidation was assessed spectrophotometrically at 532 nm by the thiobarbituric acid reaction at pH 3.5, followed by separation of MDA by solvent extraction with a mixture of n-butanol/pyridine (15:1, v/v) (32). Free F₂-isoprostanes, products of nonenzymatic peroxidation of arachidonic acid, were measured in plasma by enzyme immunoassay using 8-isoprostane kits (Cayman, Ann Arbor, MI) and a Sunrise microplate reader (Tekan, Salzburg, Austria). The results were expressed as picograms per microliter, with a detection limit of 5 pg/ml. The interassay and intraassay coefficients of variation were 9.5% and 10.7%, respectively (33). Plasma creatine kinase (CK) activity was determined by an enzymatic method (34). Protein oxidation was assessed by a spectrophotometric method for carbonyl assay (35).

Ultrastructural Studies. Electron microscopy studies of lung were carried out on 2-mm vertical slices. For transmission electron microscopy, the samples were fixed in 2.5% glutaraldehyde and 1% tannic acid in 0.1 M sodium

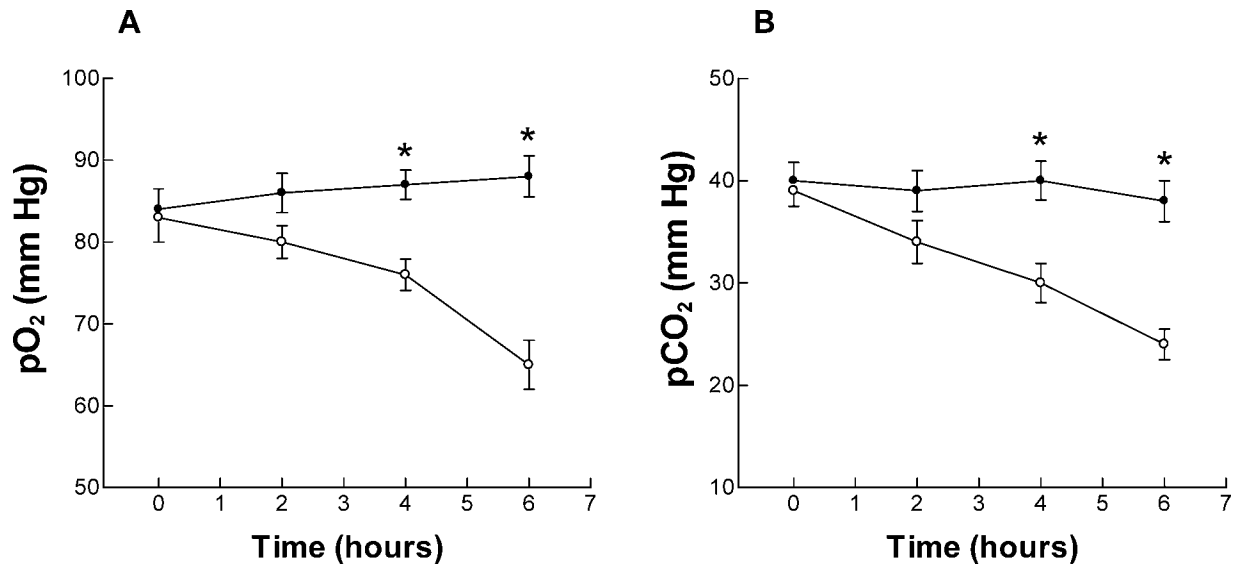


Figure 1. Effect of rhabdomyolysis on blood oxygenation (A) and blood carbon dioxide (B). Each point represents the mean \pm SEM of six animals. Open circles represent animals with rhabdomyolysis, and the closed symbols represent the matching control animals. * $P < 0.05$ compared with the control group, by ANOVA, followed by Bonferroni post hoc test.

cadodylate buffer (pH 7.3) at 4°C for 3 hrs and were post-fixed for 1 hr in 2% osmium tetroxide. The fixed samples were dehydrated in ascending grades of ethanol, cleared in propylene oxide, and embedded in EM Bed 812 epoxy resin (Electron Microscopy Sciences, Fort Washington, PA). For orientation purposes, semithin sections were stained with 1% toluidine blue in 1% sodium tetraborate and examined by light microscopy. Thin sections were prepared using a Sorvall-Porter Blum MT2-B USA ultramicrotome (Newton, CT), contrasted with uranyl acetate and lead citrate, and examined and photographed in a Zeiss EM 109 electron microscope (Zeiss, Oberkochen, Germany) (36).

Statistical Analysis. Results are expressed as the mean \pm SEM for the number of animals indicated. All statistical analyses of data were computed using Statistical Analysis System software (version 6.0; SAS Institute Inc, Cary, NC). The sources of variation for multiple comparisons were assessed by one-way analysis of variance (ANOVA), followed by Bonferroni test. The unpaired Student's *t* test was used for comparison of protein carbonylation and lipid peroxidation between the control and rhabdomyolysis groups. The differences were considered statistically significant at $P < 0.05$.

Results

Pulmonary Function Studies. Blood Gases. The time courses of PO₂ and PCO₂ changes after rhabdomyolysis induction are shown in Figure 1. Both PO₂ (Fig. 1A) and PCO₂ (Fig. 1B) were found to be significantly decreased versus controls at 4 hrs and 6 hrs following glycerol injection. Six hours after glycerol injection, arterial PO₂ and PCO₂ were 23% and 38% lower than control values ($P < 0.005$). During this period, increased heart rate and breathing frequency were noted in all animals.

Wet-to-Dry Weight Ratios. Changes in lung wet-to-dry weight ratio in response to rhabdomyolysis of the control and experimental groups are given in Table 1. At 4 hrs and at 6 hrs after glycerol injection, the ratios were significantly higher than those of the control group ($P < 0.001$).

Bronchoalveolar Lavage. Total alveolar protein in the lavage fluid (in micrograms per milliliter \times grams of dry lung⁻¹) of rats under rhabdomyolysis was significantly elevated compared with that of BAL of the control (38.5 ± 2.8 versus 26.3 ± 2.4 for rhabdomyolysis versus control, $P < 0.05$). In turn, BAL cell counts (cell numbers $\times 10^6$) (Fig. 2) revealed that the number of alveolar macrophages harvested after rhabdomyolysis was unchanged at 2 hrs, but it was increased at 4 hrs and at 6 hrs (Fig. 2A). In turn, the neutrophil count was progressively increased from 2 hrs following glycerol injection compared with the control group (Fig. 2B).

Rhabdomyolysis, Plasma Antioxidant Capacity, Lipid Peroxidation, and Protein Oxidation. As expected, glycerol injection induced rhabdomyolysis, as demonstrated by the significantly increased activity of CK in plasma at 6 hrs (0.27 ± 0.01 [$n = 8$] and 37.0 ± 1.5 [$n =$

Table 1. Time Course of Changes in Lung Wet-to-Dry Weight Ratio in Response to Rhabdomyolysis^a

Time (hrs)	Control	Rhabdomyolysis
2	5.9 ± 0.2	6.4 ± 0.3
4	6.1 ± 0.3	$7.5 \pm 0.2^*$
6	5.8 ± 0.3	$8.6 \pm 0.3^*$

^a Values are mean \pm SEM for 8 subjects.

* $P < 0.01$ compared with control group, by Student's *t* test.

RHABDOMYOLYSIS-INDUCED LUNG INJURY

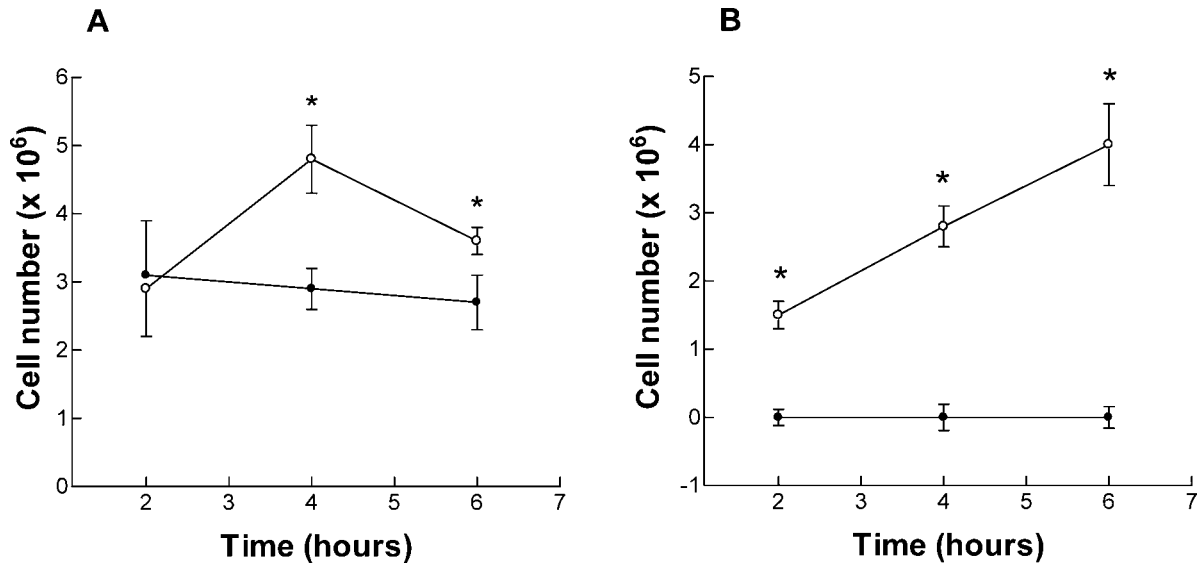


Figure 2. Effect of rhabdomyolysis on the differential cell numbers of macrophage (A) and alveolar neutrophil (B) of BAL. Each point represents the mean \pm SEM of 12 animals. Numbers are shown $\times 10^6$ cells per lung. Open circles represent animals with rhabdomyolysis, and the closed symbols represent the matching control animals. * $P < 0.05$ compared with the control group, by ANOVA, followed by Bonferroni post hoc test.

8] U/ml for control and rhabdomyolysis rats, respectively [$P < 0.05$]. Plasma antioxidant capacity, expressed as FRAP values, was significantly decreased by rhabdomyolysis (275.2 ± 4.8 [$n = 8$] and 206.4 ± 2.5 [$n = 8$] $\mu\text{M/l}$ for control and rhabdomyolysis rats, respectively [$P < 0.05$]). At this time, plasma levels of uric acid showed no significant difference between the groups (data not shown). The concomitant occurrence of oxidative stress was evidenced by plasma free F₂-isoprostane levels, which were 72% higher than those of controls (Fig. 3). In addition, the effect of rhabdomyolysis on lipid peroxidation and protein oxidation in the lung, assessed by MDA and carbonyl production, respectively, are shown in Figure 4. After glycerol injection, MDA production and protein carbon-

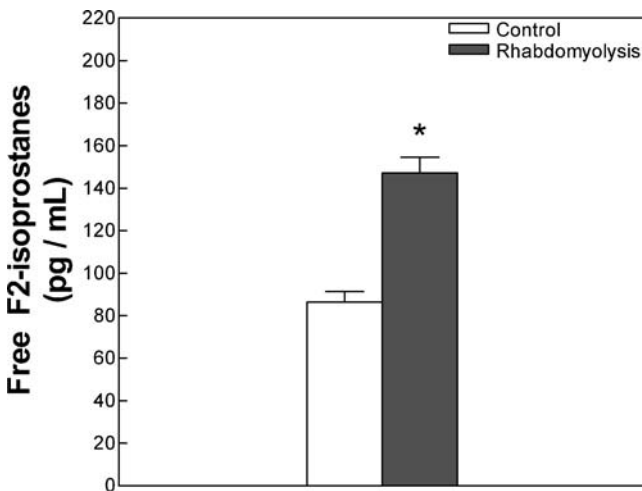


Figure 3. Effects of rhabdomyolysis on plasma lipid peroxidation products (free plasma F₂-isoprostane levels) of the rat. Bars are mean \pm SEM of eight animals. * $P < 0.05$ compared with the control group, by Student's t test.

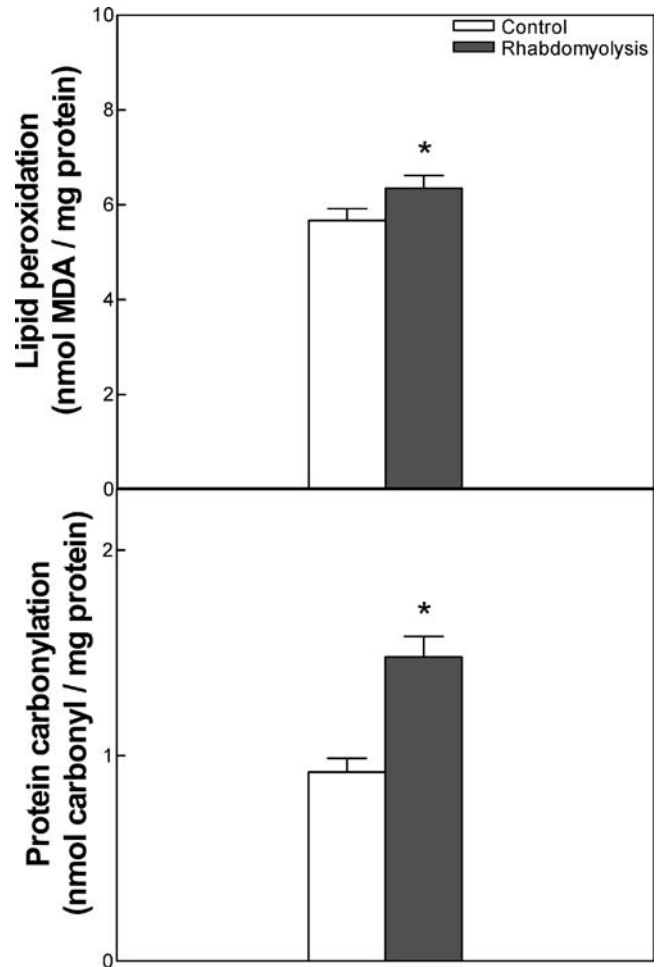


Figure 4. Effects of rhabdomyolysis on lipid peroxidation and protein carbonylation in the lung of the rat. Bars are mean \pm SEM of eight animals. * $P < 0.05$ compared with the control group, by Student's t test.

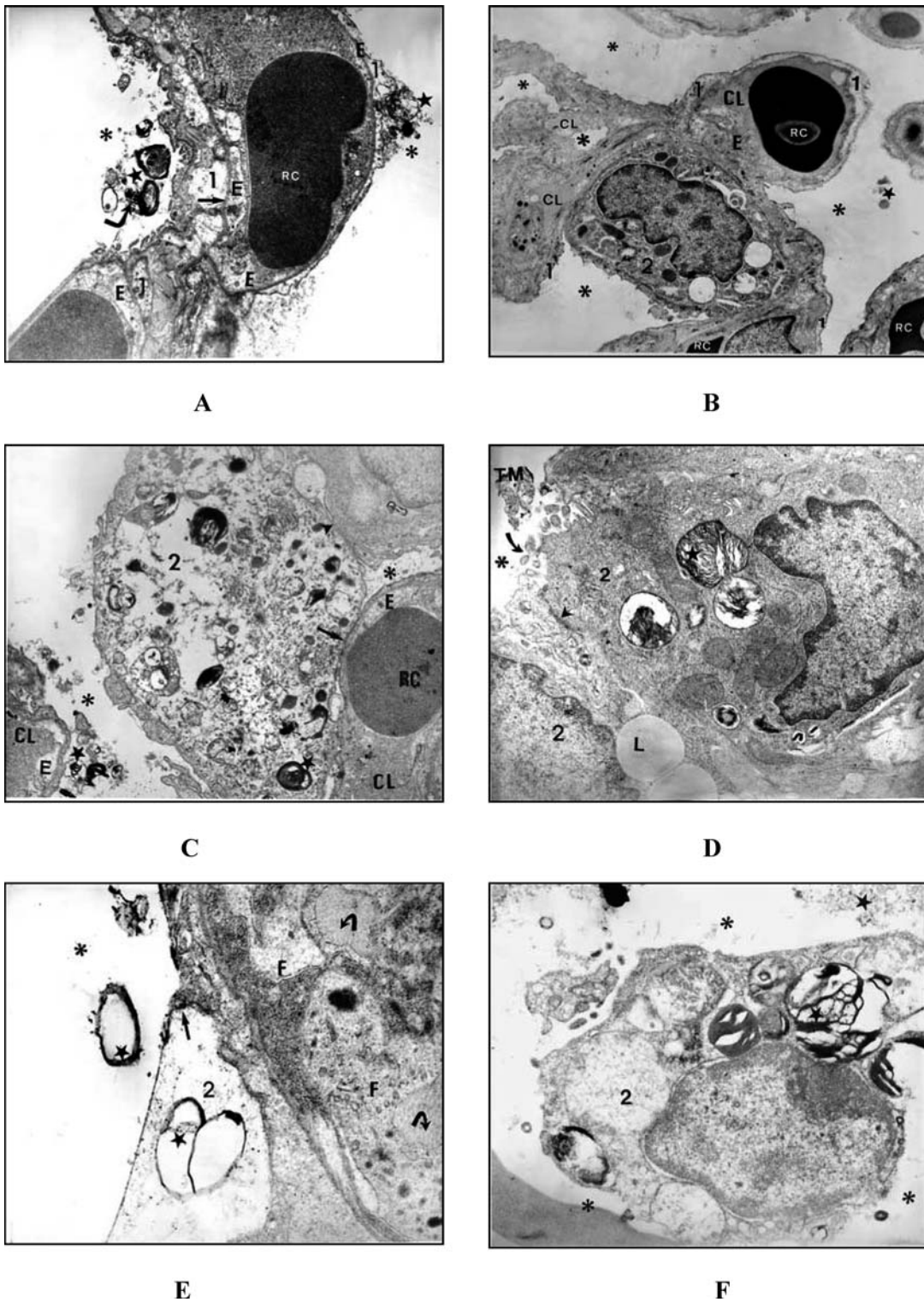


Figure 5. Electron micrographs of the lungs of rats from the control and glycerol-induced rhabdomyolysis groups. (Part A) The air-blood barrier of rats undergoing rhabdomyolysis shows cytoplasmic edema in Type I cells (1) separated by the basal membrane (arrow) from the adjacent endothelium with mild edema (E). In the alveolar lumen (*), there are numerous lamellar bodies (stars) without tubular myelin form, except the one indicated by the curved arrow. A capillary vessel is observed with a red blood cell (RC). Magnification $\times 50,000$. (Part B) Alveolar epithelium constituting the air-blood barrier of a control rat lung. One Type II cell (2) is between two Type I cells (1). One red blood cell (RC) is seen within the capillary lumen (CL). The alveolar lumen (*) is seen with surfactant (star). Magnification $\times 40,000$. (Part C) The alveolar epithelium in the lung of rats undergoing rhabdomyolysis shows injury in Type II cells (2), which are attached to the air-blood barrier by intercellular junctions, such as gap junctions and tight junctions (arrow head and arrow, respectively). Residues of lamellar bodies (star) are observed within the alveolar lumen (*), and residues of intracytoplasmic location (star) are observed in the damaged Type II cells. Edematous endothelium (E) and a red blood cell (RC) are seen in the capillary vessels (CL). Magnification $\times 50,000$. (Part D) Alveolar epithelium of a control rat lung shows two Type II cells (2),

RHABDOMYOLYSIS-INDUCED LUNG INJURY

Table 2. Effects of Rhabdomyolysis on the Content of GSH and GSSG and on the GSH:GSSG Ratio of Rat Lung^a

Variable	Control	Rhabdomyolysis
GSH ($\mu\text{mol/g}$)	0.97 \pm 0.03	0.61 \pm 0.02*
GSSG ($\mu\text{mol/g}$)	0.33 \pm 0.02	0.36 \pm 0.03
GSH:GSSG ratio	2.94 \pm 0.16	1.69 \pm 0.02*

^a Values are mean \pm SEM for 8 subjects.

* $P < 0.01$ compared with control group, by Student's *t* test.

ylation were 12% and 58%, respectively, over the control values ($P < 0.05$).

Reduced GSH and GSSG. The effect of rhabdomyolysis on the content of GSH and GSSG and on the GSH:GSSG ratio in the lung is given in Table 2. At 6 hrs following glycerol administration, GSH and the GSH:GSSG ratio had decreased by 37% and 43%, respectively.

Activity of Antioxidant Enzymes. The effect of rhabdomyolysis on the activity of the antioxidant enzymes of lung from adult rats at 6 hrs after glycerol injection is given in Table 3. The activity of GSH-Px decreased by 60% ($P < 0.05$), whereas neither SOD nor CAT showed significant changes.

Ultrastructural Characteristics. The electron micrographs of the rat lung from control and glycerol-induced rhabdomyolysis groups are shown in Figure 5. The main ultrastructural findings in the experimental group were Type II cell lysis with liberation of residues of lamellar bodies to the alveolar lumen without tubular myelin form, although these cells remained attached to the lateral cell surface by intercellular junctions. Type I cells and endothelial cells showed edema without disruption of the alveolar-capillary barrier. In the interstitium, there were increased fibroblasts with collagen fibers.

Discussion

The results presented herein provide evidence for the first time, to our knowledge, that glycerol-induced rhabdomyolysis causes ALI. Oxidative stress could be involved in mediating functional, biochemical, and ultrastructural lung changes, as increased lipid peroxidation and protein carbonylation were found at 6 hrs after intramuscular glycerol injection, whereas antioxidant capacity of plasma was significantly decreased by factors other than plasma

Table 3. Effects of Rhabdomyolysis on the Activity of the Antioxidant Enzymes CAT, SOD, and GSH-Px of Rat Lung^a

Variable	Control	Rhabdomyolysis
CAT (k/mg of protein) ^b	0.065 \pm 0.004	0.066 \pm 0.06
SOD (U/mg of protein)	6.02 \pm 0.31	6.22 \pm 0.22
GSH-Px (U/mg of protein)	0.246 \pm 0.006	0.097 \pm 0.010*

^a Values are mean \pm SEM for 8 subjects.

^b The *k* represents the CAT first-order kinetic constant for the breakdown of hydrogen peroxide ($M^{-1} \text{sec}^{-1}$).

* $P < 0.05$ compared with control group, by Student's *t* test.

levels of uric acid. It has been reported that rhabdomyolysis creates a situation with adverse effects parallel to those caused by consequences of muscle cell necrosis, contraction of intravascular volume, and heme pigment-induced acute renal failure (19, 37). The involvement of oxidative stress in the mechanism of acute renal failure by muscle necrosis has been well documented (38, 39); the oxidant renal damage is partly attributed to intrarenal iron accumulation, which is thought to be responsible for the hydroxyl radical formation (21, 40). Hence, it is possible that this mechanism could operate by increasing formation of reactive oxygen species (ROS) in different cell types, including cells other than renal cells (40). Consequently, the lung could also suffer oxidative damage. Numerous clinical observations of human diseases, as well as various experimental animal models, have demonstrated a major role of oxidative stress in the mechanism of inflammatory lung damage (41), which is in agreement with the present findings that show an early increased count of neutrophils and macrophages in BAL of rats under rhabdomyolysis (Fig. 2). These findings are very similar to those reported in an endotoxin ALI rat model (17). Despite the fact that this effect has not been considered previously (to our knowledge), the data reported herein are consistent with lung injury caused by rhabdomyolysis. Both lipid peroxidation and protein carbonylation in the lung, as well as plasma free F_2 -isoprostane levels, were all found to be increased in rats subjected to rhabdomyolysis. These findings account for the occurrence of oxidative stress in the lung and in plasma, with the latter evidenced by increased plasma F_2 -isoprostane levels.

An inappropriate response to the oxidative challenge caused by glycerol injection could account for an increased

one of them with intracellular lamellar bodies (star) and the other with intracytoplasmic lipid droplets (L). Tubular myelin (TM) in the alveolar lumen (*) is seen near the apical microvilli (arrow) of the Type II cell. Intercellular junctions (tight junctions) can be observed in the alveolar epithelium (arrow head). Magnification $\times 90,000$. (Part E) Alveolar epithelium of a rat undergoing rhabdomyolysis demonstrates considerable Type II cell lysis (2) protruding into the alveolar lumen (*) but without showing detachment. The tight junctions are preserved (arrow), while lamellar bodies on the alveolar surface of the Type II cells and intracytoplasmic ones are destroyed (stars). Two fibroblasts (F) and transversal collagen (curved arrows) are seen in the interstitium. Magnification $\times 100,000$. (Part F) Alveolar lumen (*) of a control rat lung shows a Type II cell (2). The morphology of the cell is preserved. Intracytoplasmic lamellar bodies and lamellar body residues (star) are seen within the alveolar lumen. Magnification $\times 100,000$.

vulnerability of the lung to the oxidative injury. One would expect augmented enzyme activities to defend the organism against an increase in oxidative stress. Nevertheless, we found no increased antioxidant enzyme activities in the lung of animals undergoing rhabdomyolysis, but we found decreased GSH-Px activity and a lack of increased SOD and CAT. Rhabdomyolysis causes increased ROS production via Fenton/Haber-Weiss reactions, and these species, acting as nucleophiles, are expected to exert structural damage on antioxidant proteins such as the antioxidant enzymes. Consequently, a decline in the activities of these enzymes might be due to their inactivation caused by an excess in ROS production (42). On the other hand, the molecular mechanism accounting for an antioxidant response is given by the nuclear erythroid 2 p45-related factor 2 (Nrf2), a redox-sensitive transcription factor that activates the transcription of genes encoding antioxidant enzymes (43, 44). Nrf2 binds to the promoter sequence antioxidant response element (ARE), leading to upregulation of the Nrf2-ARE pathway. It was reported that the response to ROS is profoundly impaired in Nrf2-deficient cells (44). Recently, it was demonstrated that the *GSH-Px* gene is a novel target for Nrf2 (45), and the responsiveness of Nrf2-directed antioxidant pathways may act as a major determinant of lung susceptibility to allergen-mediated asthma (46). Moreover, the alteration of GSH homeostasis is also apparent by the diminution of GSH and the GSH:GSSG ratio (Table 3), an effect consistent with an impairment of the Nrf2-ARE pathway that has recently been reported to play a role in the regulation of glutamylcysteine ligase, the rate-limiting enzyme in GSH synthesis (47), also in agreement with the impaired response of this antioxidant defense pathway in the regulation of antioxidant enzymes. However, further studies are needed to test the hypothesis of a role for Nrf2 in the antioxidant response of the lung in the model of rhabdomyolysis-induced oxidative stress. It should be noted that the GSH decrease was not accompanied by a GSSG increase, which could be due to effects of GSH and GSSG efflux out of the cell, reduced GSH lung uptake or synthesis, and/or GSH depletion by both ROS and GSH-Px-catalyzed reaction.

The functional effects of rhabdomyolysis on the lung in this model have not been previously reported, to our knowledge. Our data showing gas exchange impairment and pulmonary edema (endothelial and Type I cells) suggest the initiation of an inflammatory process likely mediated by oxidative stress. In addition, the presence of increased protein concentration and neutrophil count and increased macrophage count in BAL at 4 hrs after glycerol injection could contribute to the development of the effects on lung function. Thus, despite the increased breathing frequency shown by the animals following glycerol injection, decreased PCO₂ was accompanied by decreased PO₂ (Fig. 1), likely due to a differential effect of the production of pulmonary edema on the diffusion of both gases, with that of O₂ being particularly affected by the impairment of the air-

blood barrier (Fig. 5). In contrast, the increased ventilation causes hypocapnia due to the easier diffusion of CO₂. Together with the occurrence of edema in endothelial and Type I cells, the induction of pulmonary edema is further supported by data demonstrating an increased lung wet-to-dry weight ratio in response to rhabdomyolysis (Table 1), an effect especially relevant at 6 hrs following glycerol injection. However, further studies, including permeability assessment, and a longer period of observation would be valuable to corroborate this hypothesis.

The ultrastructural findings showing physical distortion of Type II cells, likely due to the effect of lipid peroxidation on membrane phospholipids, are consistent with an impairment of surfactant secretion and turnover. This assumption is further supported by the presence of lamellar body residues within the alveolar lumen (Fig. 5C), which could contribute to the functional effect on O₂ diffusion (Fig. 1), in agreement with data reported in other experimental models of ALI (17, 48).

Epidemiological investigations have shown that patients with trauma had a 25.5% overall incidence of ARDS (49). Nevertheless, ARDS is frequently associated with other clinical risk factors, such as sepsis, gastric aspiration, and multiple transfusions, known to increase the development of ARDS, with a high mortality (20, 38). No attempts to analyze the association between rhabdomyolysis and ARDS have been made previously, to our knowledge. However, the occurrence of oxidative stress in ARDS is well documented (15, 16). F₂-isoprostanes have been reported to be as high as 10-fold in the exhalation breath condensate of patients with ARDS (13, 15). The present data showing biochemical features of plasma and lung oxidative stress associated with morphological lung alterations provide some proof that the lung is an organ that undergoes oxidative damage during rhabdomyolysis. Therefore, it may be suggested that an element of the metabolic derangement of the lung operates in the mechanism of ARDS in patients with the direct or indirect muscle necrosis associated with ARDS. In our descriptive ultrastructural studies (Fig. 5), the air-blood barrier is altered due to endothelial and Type I cell edema as well as lysis in numerous Type II cells, thereby obstructing their stem function and thus their mitotic progeny (36). This alteration is very similar in hyperoxia or acute ethanol exposure in the lung (10, 11), but in these models the cell adhesion tight and gap junctions are not disrupted. Oxidation damage of DNA can probably include apoptosis in lung cells (50), thus explaining the functional changes. For example, in the model used in the present study, surfactant is present on the alveolar surface but not as tubular myelin (36), indicating that the mechanism for its secretion may have been modified. Further studies involving pulmonary function related to oxidative stress and other morphological parameters, as well as assessment of surfactant turnover, should be carried out to better understand these findings.

In summary, these data support the view that

RHABDOMYOLYSIS-INDUCED LUNG INJURY

rhabdomyolysis induced by glycerol may cause biochemical, functional, and ultrastructural lung damage associated with and likely mediated by increased oxidative stress, as occurs in other organs, thereby providing some insights for the pathogenic mechanism of ARDS in patients with muscle injury.

- Gattinoni L, Pelosi P, Suter P, Pedoto A, Vercesi P, Lissoni A. Acute respiratory distress syndrome caused by pulmonary and extrapulmonary disease: different syndromes? *Am J Respir Crit Care Med* 158:3–11, 1998.
- Ware LB, Matthay MA. The acute respiratory distress syndrome. *N Engl J Med* 342:1334–1349, 2000.
- Stricter RM, Steven LK, Keane PM, Standford TJ. Chemokines in lung injury. *Chest* 116:103S–110S, 1999.
- Warshawski J, Sibbald WJ, Driedger AA, Cheung H. Abnormal neutrophil-pulmonary interaction in the adult respiratory distress syndrome. *Am Rev Respir Dis* 133:797–804, 1986.
- Suter PM, Suter S, Girardin E, Roux-Lombard P, Grau GE, Dayer JM. High bronchoalveolar levels of tumor necrosis factor and its inhibitors, interleukin-1, interferon, and elastase, in patients with adult respiratory distress syndrome, after trauma, shock, or sepsis. *Am Rev Respir Dis* 145:1016–1022, 1992.
- Donnelly SC, MacGregor I, Zamani A, Gordon MW, Robertson CE, Steedman DJ, Little K, Haslett C. Plasma elastase in multiple trauma and the adult respiratory distress syndrome (ARDS). *Am J Respir Crit Care Med* 151:1428–1433, 1995.
- Christner P, Fein A, Goldberg S, Lippmann M, Abrams W, Weinbaum G. Collagenase in the lower respiratory tract of patients with adult respiratory distress syndrome. *Am Rev Respir Dis* 131:690–695, 1995.
- Donnelly SC, MacGregor I, Zamani A, Gordon MW, Robertson CR, Carter DC, Grant IS, Pollok AJ, Haslett C. Interleukin 8 (IL-8) and the development of the adult respiratory distress syndrome (ARDS) in at risk patient groups. *Lancet* 341:643–647, 1993.
- Barazzone C, White CW. Mechanisms of cell injury and death in hyperoxia: role of cytokines and Bcl-2 family proteins. *Am J Respir Cell Mol Biol* 22:517–519, 2000.
- Piedbouf B, Frenette J, Petrov P, Welty SE, Kazzaz J, Horowitz S. *In vivo* expression of intercellular adhesion molecule 21 in type II pneumocytes during hyperoxia. *Am J Respir Cell Mol Biol* 15:71–77, 1996.
- Rodrigo R, Trujillo S, Bosco C, Orellana M, Thielemann L, Araya J. Changes in (Na + K)-adenosine triphosphatase activity and ultrastructure of lung and kidney associated with oxidative stress induced by acute ethanol intoxication. *Chest* 121:589–596, 2002.
- Cross CE, Valacchi G, Schock B, Wilson M, Weber S, Eiserich J, van der Vliet A. Environmental oxidant pollutant effects on biologic systems: a focus on micronutrient antioxidant-oxidant interactions. *Am J Respir Crit Care Med* 166(Pt 2):S44–S50, 2002.
- Janssen LJ. Isoprostanes: an overview and putative roles in pulmonary pathophysiology. *Am J Physiol Lung Cell Mol Physiol* 280:L1067–L1082, 2001.
- Morrow JD, Roberts LJ. The isoprostanes: their role as an index of oxidant stress status in human pulmonary disease. *Am J Respir Crit Care Med* 166(Pt 2):S25–S30, 2002.
- Carpenter CT, Price PV, Christian BW. Exhaled breath isoprostanes are elevated in patients with lung injury and ARDS. *Chest* 114:1653–1659, 1998.
- Pacht ER, Timmerman AP, Lykens MG, Merola AJ. Deficiency of alveolar glutathione in patients with sepsis and the adult respiratory distress syndrome. *Chest* 100:1397–1403, 1991.
- Davidson KG, Bersten AD, Barr HA, Dowling KD, Nicolas TE, Doyle IR. Endotoxin induces respiratory failure and increases surfactant over and respiration independent of alveolocapillary injury in rats. *Am J Respir Crit Care Med* 165:1516–1525, 2002.
- Safdar Z, Yiming M, Grunig G, Bhattacharya J. Inhibition of acid-induced lung injury by hyperosmolar sucrose in rats. *Am J Respir Crit Care Med* 172:1002–1007, 2005.
- Zager R. Rhabdomyolysis and myohemoglobinuric acute renal failure. *Kidney Int* 49:314–326, 1996.
- Warren JD, Blumberg PC, Thompson PD. Rhabdomyolysis: a review. *Muscle Nerve* 25:332–347, 2002.
- Zager R. Mitochondrial free radical production induces lipid peroxidation during myohemoglobinuria. *Kidney Int* 49:741–751, 1996.
- Sharkey RA, Donnelly SC, Connelly KG, Robertson CE, Haslett C, Repine JE. Initial serum ferritin levels in patients with multiple trauma and the subsequent development of acute respiratory distress syndrome. *Am J Respir Crit Care Med* 159:1506–1509, 1999.
- Grossman R, Hamilton R, Morse B, Penn A, Goldenberg M. Non-traumatic rhabdomyolysis and acute renal failure. *N Engl J Med* 291:807–811, 1974.
- Parker JC, Townsley MI. Evaluation of lung injury in rats and mice. *Am J Physiol Lung Cell Mol Physiol* 286:L231–L246, 2004.
- Taylor MD, Antonini JM, Roberts JR, Leonard SS, Shi X, Gannett PM, Hubbs AF, Reasor MJ, Taylor MD, Antonini JM, Roberts JR, Leonard SS, Shi X, Gannett PM, Hubbs AF, Reasor MJ. Intratracheal amiodarone administration to F344 rats directly damages lung airway and parenchymal cells. *Toxicol Appl Pharmacol* 188:92–103, 2003.
- Lowry OH, Rosebrough NJ, Farr AL, Randall RJ. Protein measurement with the folin phenol reagent. *J Biol Chem* 193:265–275, 1951.
- Nebot C, Moutet M, Huet P, Xu JZ, Yadan JC, Chaudiere J. Spectrophotometric assay of superoxide dismutase activity based on the activated autooxidation of a tetracyclic catechol. *Anal Biochem* 214:442–451, 1993.
- Aebi H. Catalase. In: Bergmeyer HU, Ed. *Methods in Enzymatic Analysis* (29th ed.). New York: Academic Press, p673, 1974.
- Flohé L, Günzler W. Assays of glutathione peroxidase. In: Colowic S, Kaplan N, Eds. *Methods in Enzymology*. New York: Academic Press, Vol 105:p114, 1984.
- Hissin PJ, Hilf RA. A fluorometric method for determination of oxidized and reduced glutathione in tissues. *Anal Biochem* 74:214–226, 1976.
- Benzie IFF, Strain JJ. The ferric reducing ability of plasma (FRAP) as a measure of “antioxidant power”: the FRAP assay. *Anal Biochem* 239:70–76, 1996.
- Ohkawa H, Ohishi N, Yagi K. Assay for lipid peroxides in animal tissues by thiobarbituric acid reaction. *Anal Biochem* 95:351–358, 1979.
- Pradelles P, Grassi J, Maclouf J. Enzyme immunoassays of eicosanoids using AchE as label: an alternative to radioimmunoassay. *Anal Chem* 57:1170–1173, 1985.
- Burtis CA, Ashwood ER, Eds. *Tietz Textbook of Clinical Chemistry* (2nd ed.). Philadelphia: WB Saunders, pp797–799, 1994.
- Reznick AZ, Packer L. Oxidative damage to proteins: spectrophotometric methods for carbonyl assay. In: Colowic SP, Kaplan NO, Eds. *Methods in Enzymology*. New York: Academic Press, Vol 233:p357, 1994.
- Scharaufnagel D. *Electron Microscopy of the Lung*. New York: Marcel Dekker, p180, 1990.
- Sauret JM, Marinides G. Rhabdomyolysis. *Am Fam Physician* 65:907–912, 2002.
- Matthew S, Mullins R. Rhabdomyolysis and myoglobinuric renal

- failure in trauma and surgical patients: a review. *J Am Coll Surg* 186: 693–716, 1998.
39. Sulowicz W, Walatek B, Sydor A, Ochmanski W, Miłkowski A, Szymczakiewicz-Multanowska A, Szumilak D, Krasniak A, Łonak H, Wojcikiewicz T. Acute renal failure in patients with rhabdomyolysis. *Med Sci Monit* 81:CR24–CR27, 2002.
 40. Paller MS, Hoidal JR, Ferris TF. Oxygen free radicals in ischemic acute renal failure in the rat. *J Clin Invest* 74:1156–1164, 1984.
 41. Soejima K, Traber LD, Schmalstieg FC, Hawkins H, Jodoin JM, Szabo C, Szabo E, Varig L, Salzman A, Traber DL. Role of nitric oxide in vascular permeability after combined burns and smoke inhalation injury. *Am J Respir Crit Care Med* 163:745–752, 2001.
 42. Pigeolet E, Corbisier P, Houbion A, Lambert D, Michiels C, Raes M, Zachary MD, Remacle J. Glutathione peroxidase, superoxide dismutase, and catalase inactivation by peroxides and oxygen derived free radicals. *Mech Ageing Dev* 51:283–297, 1990.
 43. Lee JM, Li J, Johnson DA, Stein TD, Kraft AD, Calkins MJ, Jakel RJ, Johnson JA. Nrf2, a multi-organ protector? *FASEB J* 19:1061–1066, 2005.
 44. Ishii T, Itoh K, Takahashi S, Sato H, Yanagawa T, Katoh Y, Bannai S, Yamamoto M. Transcription factor Nrf2 coordinately regulates a group of oxidative stress-inducible genes in macrophages. *J Biol Chem* 275: 16023–16029, 2000.
 45. Banning A, Deubel S, Kluth D, Zhou Z, Brigelius-Flohé R. The *GI-GPx* gene is a target for Nrf2. *Mol Cell Biol* 25:4914–4923, 2005.
 46. Rangasamy T, Guo J, Mitzner WA, Roman J, Singh A, Fryer AD, Yamamoto M, Kensler TW, Tuder RM, Georas SN, Biswal S. Disruption of Nrf2 enhances susceptibility to severe airway inflammation and asthma in mice. *J Exp Med* 202:47–59, 2005.
 47. Rahman I. Regulation of glutathione in inflammation and chronic lung diseases. *Mutat Res* 579:58–80, 2005.
 48. Davidson KG, Bersten AD, Barr HA, Dowling KD, Nicholas TE, Doyle IR. Lung function, permeability and surfactant composition in oleic acid-induced acute lung injury in rats. *Am J Physiol Lung Cell Mol Physiol* 279:L1091–L1102, 2000.
 49. Matthay MA, Zimmerman G. Acute lung injury and the acute respiratory distress syndrome: four decades of inquiry into pathogenesis and rational management. *Am J Respir Cell Mol Biol* 33:319–327, 2005.
 50. Albertine KH, Plopper CG. DNA oxidation apoptosis: will the real culprit of DNA damage in hyperoxic lung injury please stand up? *Am J Respir Cell Mol Biol* 26:381–383, 2002.